Separation Science and Technology
Publication details, including instructions for authors and subscription information:
http://www.informaworld.com/smpp/title~content=t713708471

Gas Separation Properties of Phosphazene Polymer Membranes

R. R. Mccaffrey[a]; D. G. Cummings[a]
[a] Idaho National Engineering Laboratory, EG&G Idaho, Inc., Idaho Falls, Idaho

To cite this Article Mccaffrey, R. R. and Cummings, D. G.(1988) 'Gas Separation Properties of Phosphazene Polymer Membranes', Separation Science and Technology, 23: 12, 1627 — 1643
To link to this Article: DOI: 10.1080/01496398808075653
URL: http://dx.doi.org/10.1080/01496398808075653

SEPARATION SCIENCE AND TECHNOLOGY, 23(12&13), pp. 1627-1643, 1988

GAS SEPARATION PROPERTIES OF PHOSPHAZENE POLYMER MEMBRANES

R. R. McCaffrey and D. G. Cummings
Idaho National Engineering Laboratory, EG&G Idaho, Inc.
P. O. Box 1625
Idaho Falls, Idaho 83415

ABSTRACT

In this paper the gas separation properties of poly[bis(phenoxy)phosphazene] are reported. Transport behavior was determined by time-lag techniques and correlated with membrane microstructural studies. Test gases were run as pure or single-species gases, which included atmospheric gases, hydrocarbons, sulfur dioxide, and hydrogen sulfide. Transport of atmospheric and hydrocarbon gases was found to be a diffusion controlled process; i.e., correlated with molecular size. Transport of CO_2, H_2S, and SO_2 was found to be a sorption controlled process since high solubilities were measured and transport deviated from the diffusion controlled permeability-size correlation. Membranes were prepared using spin and knife casting techniques. Solvent evaporation rate during the casting process was used to provide different membrane microstructures. Rapid evaporation by spin casting resulted in dense homogeneous films, with permeabilities ranging from 2-6 barrers for the slowest (Ar) to fastest gases (He). Slow evaporation by knife casting (minutes-hours) resulted in a more open polymer structure. Two enhancement effects were observed in the transport behavior of the knife-cast membrane: 1) an overall increase in permeability for all gases depicting the more open membrane structure (ranged from 4-76 barrers for all gases) and 2) an enhancement of the selectivity of gases which exhibited strong solubility effects. Sulfur dioxide and hydrogen sulfide exhibited the greatest selectivity enhancements. The pure gas solubility selectivities for SO_2 and H_2S with respect to the atmospheric and hydrocarbon gases were found to be approximately 1000 and 200 respectively.

INTRODUCTION

Rising energy costs and environmental concerns in recent years have resulted in increasing efforts in both the industrial and government sectors for the development of energy efficient separation processes. One of these efforts, at the Department of Energy's Idaho National Engineering Laboratory (INEL), is the Inorganic Membrane Technology Research Program (IMTRP). At present, the IMTRP is supported by the Department of The Interior's Bureau of Mines as part of the Strategic and Critical Materials Program. The current thrust of the IMTRP, based on the Bureau of Mines concerns and industrial needs identified in a recent DOE report (1), is the development of energy efficient separation processes. Specific Bureau interests include: 1) recovering strategic and critical materials from hydrometallurgical operations and; 2) removing environmentally harmful gases from smelting and roasting operations.

One apparent answer to these processing needs is the use of membranes. Since membrane processes are non-energy intensive compared to traditional phase separation processes, they could offer significant energy savings for the extraction processes. The immediate problem, however, is that available commercial organic membrane systems would degrade in the adverse thermal (>100^{o}C) and chemical (extreme pH) environments frequently encountered in these operations.

An alternative, proposed by the INEL, is the use of phosphazene polymers as membranes. The phosphazene polymers were proposed for the Bureau of Mines applications since many phosphazene polymers have the required thermal and chemical stabilities. The objective of the present program is to develop, characterize, and test a variety of inorganic based, high temperature, separation membranes applicable to strategic and critical materials processing and waste gas stream conditioning. The results presented in this paper address waste gas stream conditioning. Initial emphasis has been directed to the separation of sulfur dioxide and hydrogen sulfide from roasting off-gas streams. Liquid diffusion studies on separating strategic and critical materials in hydrometallurgical operations are reported elsewhere (2,3).

The pure gas transport behavior of poly[bis(phenoxy) phosphazene] is reported in this paper. Membranes were prepared by spin and knife casting techniques. The rate of solvent evaporation in the two casting techniques was used to prepare membranes with different microstructures. Optical and electron microscopic techniques were used to characterize the membrane microstructure. Gas permeation studies included determination of permeability, diffusivity, and solubility as a function of test gas and membrane microstructure using the time-lag permeation technique. Test gases included atmospheric gases,

hydrocarbons, carbon monoxide, carbon dioxide, sulfur dioxide, and hydrogen sulfide. Membrane microstructure studies were correlated with the permeation studies to determine the controlling factors of transport in the phosphazene membrane.

Background. Phosphazene polymers consist of alternate phosphorus-nitrogen single and double bonds in the polymer backbone with two side groups attached to the phosphorus atoms (4). These polymers can be easily modified with a variety of side groups by nucleophilic substitution and exchange reactions. Three types of polyphosphazene backbone structures (linear, cyclolinear, and cyclomatrix) provide flexibility in modifying the thermal, chemical, and mechanical properties. Linear organo-substituted polyphosphazene is synthesized by ring-cleavage polymerization of a cyclic trimer (usually hexachlorocyclotriphosphazene) at 250°C under vacuum, and subsequent substitution with the desired side group. Cyclolinear and cyclomatrix polymers are prepared by reacting the cyclic trimer with difunctional monomers. The type of polymer obtained is dependent on the mole ratio of the reactants and reactive sites on the trimer. Chemical and thermal properties of the polymers are related to both the polymer backbone structure and side groups (5).

Membrane Studies. There are essentially two ways to evaluate the transport characteristics of a membrane material; one is to do a mixed gas study and the other a pure gas study. To evaluate an unknown membrane material by a mixed gas study, a large number of gas mixture combinations are required to get an overall picture of the membrane transport behavior. A pure gas study requires testing only the gases of interest; results are used to predict the behavior of specific mixtures.

The time-lag pure gas permeation technique was chosen for investigation of gas transport in phosphazene polymers. The time-lag pure gas permeation technique is considered a static technique in which the gas flow across the membrane is measured as a pressure rise with time on the permeate side of the membrane (6-9). The gas transport parameters determined in this experiment include permeability (P) and diffusivity (D); solubility can be calculated from P and D. The advantage of the technique stems from its simplicity; no gas analysis is required for the pure gas study and boundary effects are essentially eliminated. In addition, the technique permits the calculation of P, D, and S in one experiment. The disadvantages include sensitivity to pressure and temperature fluctuations, and concentration dependent effects. The first two can be eliminated with proper care to apparatus design and the latter can be reduced at low gas concentrations or high temperatures.

A pictorial representation of the time-lag technique is shown in Figure 1. After the test gas is introduced at the feed

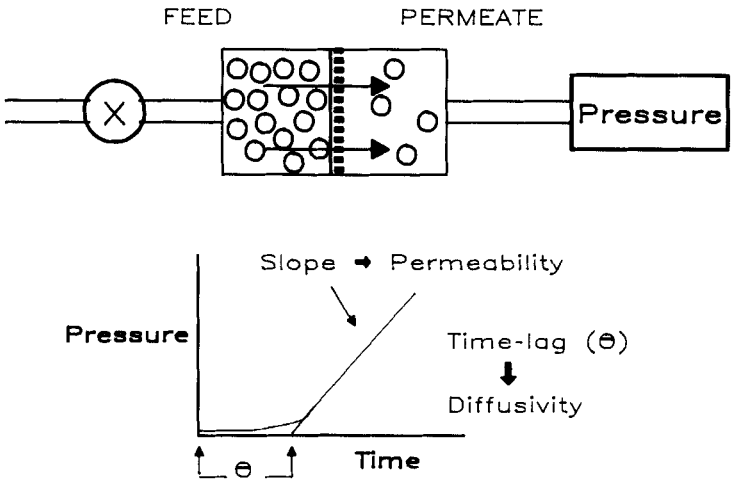

Figure 1.0 Pictorial representation of time-lag gas permeation technique.

side of the membrane, gas flow across the membrane is measured on the permeate side as a pressure rise with time. A typical pressure-time plot is shown in the lower portion of Figure 1. The pressure-time plot usually consists of two regions: a linear and a nonlinear region. The linear region occurs when gas flow across the membrane has reached a steady state value. The slope of the linear region is related to the permeability. Expressed in terms of a pressure increase per unit time at STP conditions, the permeability is:

$$\bar{P} = \frac{\Delta p_2}{\Delta t} * \frac{V_2}{T} * \frac{L}{p_1 A} * \frac{T_s}{p_s} \qquad -1-$$

where T_s and p_s are temperature and pressure at standard conditions, p_1 is the feed pressure, p_2 is the permeate pressure, V_2 is the permeate test cell volume, T is the absolute temperature, A is the membrane area, L is the membrane thickness, and t is time. When the test gas is first introduced into the feed side of the membrane, a short build-up period occurs before the flow rate reaches steady state. This results in the nonlinear region of the p-t plot. This build-up period is called the time lag and is used to calculate the apparent diffusivity. For a thin planar membrane with defined boundary conditions, the time-lag expression for the apparent diffusion coefficient, derived from the solution to Fick's diffusion equation, is given as: (8,9)

$$\bar{D}_a = L^2/6\theta \qquad -2-$$

where θ is the time lag. Using the permeability and diffusivity values obtained from the time-lag measurements, solubility can be calculated from the permeability equation:

$$\bar{P} = \bar{D}_a \bar{S}. \qquad -3-$$

EXPERIMENTAL

Synthesis. Poly[bis(phenoxy)phosphazene] (PPOP) was prepared using a modification of Singlers' procedure (10). The synthesis route for PPOP is:

$$[\text{-N=P(Cl)}_2\text{-}]_n + 2n\ \text{NaOC}_6\text{H}_5 \xrightarrow[\text{dark 42 h}]{\text{reflux 110}^\circ\text{C}} [\text{-N=P(OC}_6\text{H}_5)_2\text{-}]_n + 2n\ \text{NaCl}.$$

Details of the procedure have been previously reported (3,11). Yields of 50-60% were achieved with this method. The resulting polymer solid was a white, fibrous, flexible, film-forming material which dissolved easily in tetrahydrofuran.

Polymer molecular weights were determined by gel permeation chromatography (GPC) using a Kratos HPLC system with a refractive index detector. Two DuPont trimodal silanized PS columns connected in series were used with a tetrahydrofuran flow rate of 1.0 ml/min. The columns were calibrated by means of narrow distribution polystyrene standards obtained from DuPont. Molecular weights were calculated using the ASTM universal calibration method (12). The number and weight average molecular weights for PPOP were 75,000 daltons and 350,000 daltons respectively.

Casting. Membranes were prepared by both spin and knife casting techniques from a prefiltered 4.3% PPOP solution of tetrahydrofuran (THF). The casting procedure was the same for both techniques; membranes were cast on glass plates, dried (24 hours), floated off the glass substrates onto water, transferred to a porous test cell support, and edge-sealed to the support with polymer solution. The spin caster was a modified Dynac benchtop centrifuge with a casting platform. Glass casting plates were secured to the casting platform during operation by double sticky tape. The knife apparatus consisted of a glass balance platform and glass knife rod. The glass balance platform was balanced with three micrometer adjusting screws and a leveling bulb to provide a level casting surface. The glass knife rod was used to define solution heights during casting, and tape layers applied to the end of the knife rod defined knife

height (the tape thickness was 60 μm). Six layers of tape were used on the knife rod to provide a knife height of 360 μm. Film thickness was determined by optical microscopic techniques using a calibrated reticle (Riechert AO microscope). Electron microscopic techniques were used to evaluate membrane surface structure and thickness of thin membranes. The TEM instrument was a Philips EM 420 STEM operated at 120 kV. The TEM membrane samples were prepared on 3 mm diameter copper grid discs (grid holes were 100 μm square). All polymer samples were coated with either gold or carbon films (~ 10 nm) to reduce charging effects on the polymer surface.

Testing. The gas transport behavior of the PPOP membrane was determined using a time-lag gas permeation test cell fabricated at the INEL (11). Both the feed and permeate sides of the test cell were connected to a vacuum line to enable complete desorption before starting each experiment. Feed pressure was monitored with a 0-100 psi (0-7 bar) absolute pressure transducer, and permeate pressure was monitored with a MDC Vacuum Products Corporation vacuum thermocouple gauge and a MKS Instruments 0-10 mm Hg differential pressure transducer. The reference part of the differential transducer was evacuated with a Sargent Welsh oil vacuum pump.

An Analog Device Macsym 2 computer system was interfaced to the time-lag apparatus to control the apparatus, data acquisition, and data analysis. The software, written in BASIC, consisted of three parts: a control section, data acquisition section, and data analysis section. The control section was used to open and close four solenoid pressure actuator valves during the experiment; namely, 1) permeate vacuum valve, 2) feed vacuum valve, 3) feed exhaust valve, and 4) sample gas valve. The cell temperature and pressures were measured during data acquisition. Permeabilities and time lags were calculated from this data. System lags, measured for all the test gases, ranged from 0.2-0.4 seconds. Membrane time lags were corrected for system lags prior to the calculation of D and S. Since membrane time lags for the fast diffusing gases were of the same order of magnitude as the system time lags, 50-100% errors were estimated for the membrane time lag and, consequently, D and S. In the case of CO_2, H_2S and SO_2, membrane time lags were at least 1-2 orders in magnitude greater than system lags. The membrane time lag error for these gases is expected to be much smaller.

RESULTS AND DISCUSSION

In addition to the physicochemical properties of a polymer material, the membrane polymer morphology or microstructure affects the membrane's gas transport properties. To a large extent the membrane polymer morphology can be defined and controlled in the membrane preparation steps. Depending on casting conditions, several different types of membrane

morphologies can be formed, each exhibiting a unique set of transport characteristics. Specific examples include dense nonporous membranes formed from single solvent systems, porous membranes formed from solvent systems doped with pore-forming salts, or asymmetric membranes formed from solvent/nonsolvent systems and solvent quenching.

The objective of this study was to gain an overall understanding of the transport behavior of the PPOP membrane. To accomplish this, a dense nonporous homogeneous membrane structure was chosen for initial study. In choosing the nonporous membrane, it was hoped that complications in transport behavior due to Knudsen and Pousieulle contributions would be eliminated and that transport behavior would be due only to a solution diffusion process with the membrane.

Membrane Microstructure. Dense nonporous structures of PPOP were prepared by solvent casting techniques using single solvents. The membranes were prepared by both the knife and spin casting techniques as described in the Experimental section. In keeping all process parameters constant (film thickness, polymer concentration, and temperature), the main difference between the spin and knife casting techniques is solvent evaporation time, which is on the order of seconds for the spin casting technique and minutes to hours for knife casting. The spin cast technique removes solvent rapidly and can be thought of as a quench casting technique, which results in dense membranes. The knife casting technique can involve long evaporation times, which allows polymer/solvent equilibrium to be maintained and results in large open polymer structure (13).

Three types of polymer films were prepared using a solution of 4.3% PPOP in THF. One film was prepared by the spin casting technique and the other two by a knife technique; solvent evaporation times were altered for each film. Details of the casting conditions are given in Table I. The effect of solvent evaporation time on membrane microstructure was examined in this study. The effects of microstructure on transport properties are discussed in the next section.

The results (Table I) show that larger polymer structure, either pores or spherulites, is formed with increasing evaporation time. This is evident from the loss of clarity from micrographs of PPOP4A to PPOP4C, which is due to scattering of visible light by large structure in the membrane. Optical photomicrographs of the three films are shown in Figure 2.

Figure 2d shows a TEM photomicrograph of a spin cast film (~200 nm thick; PPOP4A) at a hole defect in the thin film. This photomicrograph, taken at 600,000 magnification, shows the presence of microstructure within the membrane. There are two possible explanations for this structure; one is the presence of

TABLE I. Solvent evaporation times and casting conditions for PPOP films prepared from 4.3% THF solution of PPOP.

Sample Method	Evaporation Time	Thickness (μm)	Observations
PPOP4A Spin cast	<5seconds	~10	Transparent, no visible micro structureat 100 mag.
PPOP4B Knife cast	~30min	15	Translucent, small circular microsture 10-20 μm at 100 mag.
PPOP4C Knife cast	~2h	~50	White translucent large circular surface structure 40-60 μm at 100 mag.

gold and the other is the presence of polymer. The first possibility is that the structure is entirely due to gold, since the polymer was coated with a 10 nm gold film to reduce charging effects. Such structures are common for thin gold films (14). Electron diffraction and dark field studies were performed to confirm the presence of gold. The electron diffraction patterns generated from these films were consistent with the diffraction patterns of gold aggregates, i.e., sharp concentric rings. Dark field experiments indicated that the diffracted signal was due only to diffraction through the dark spots in the photomicrograph and not in the bulk of the film. Since most of the spots did not contribute to the diffraction signal, it is possible that they could be caused by amorphous gold.

Another explanation for this structure is polymer crystallites. Three observations make this explanation seem plausible: 1) expected structure from spin cast, 2) molecular dimensions and molecular weight, and 3) alignment of structures within the photomicrograph. As a result of rapid solvent evaporation in the spin cast technique, the membrane microstructure is expected to consist of small crystallites with no long-range order (13). This appears to be the case as observed in the PPOP4A photomicrographs. In addition, the size

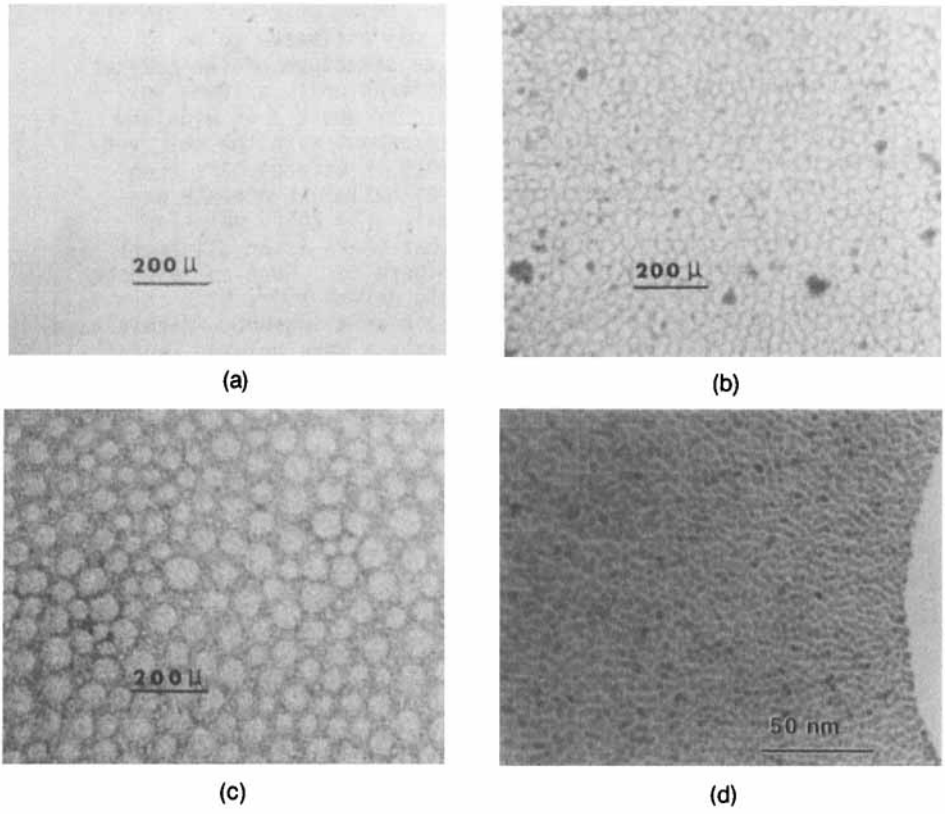

Figure 2.0 Optical and electron photomicrographs of PPOP films with differing solvent evaporation times; (a)-PPOP4A, spin cast, evaporation time <5 seconds; 2(b)-PPOP4B, knife cast, evaporation time 30 minutes; 2(c)-PPOP4C, knife cast, evaporation time 2 hours; 2(d)-PPOP4A, Transmission electron photomicrograph.

of the structures in Figure 2d seem to match molecular dimensions of PPOP quite well. These structures are about 5 nm wide, 50-100 nm long, and 1 nm apart (distance between dark areas). Based on an average molecular weight of 200,000 daltons (from M_n = 75,000 daltons and M_w = 350,000 daltons; determined by GPC) and a monomeric repeat distance of 0.49 nm (15), an average PPOP4 chain would be 500 nm long if stretched as a rigid rod. Such a configuration for most polymer systems, however, is not typical. Instead, a more reasonable configuration of the polymer would be

a chain-folded lamellae crystallite. Using unit cell data for PPOP, the width of a monomeric unit was estimated to be 0.5-1.0 nm (15). Assuming a lamellae structure of the polymer and molecular dimensions of the monomeric unit, a lamellae structure of 5-10 folded chains would be about 5 nm wide and 50-100 nm long, which is in close agreement with the observed dimensions in Figure 2. Similar dense structures have been reported for quench cast membranes of cellulose acetate and described as crystalline nodules (13). The third point of the polymer structure argument is that there is an alignment of structure radially to the hole in Figure 2d. Such an alignment is expected for a polymer near a hole defect since high stresses encountered in that region would favor an alignment. Examination of structure away from the hole reveals a more relaxed random orientation.

As a result of these observations it is believed that the structure of Figure 2d is due either to polymer or a reflection by gold of the underlying polymer structure. Further TEM and SEM studies are in progress to draw a positive conclusion. Regardless of whether the structure of Figure 2d is polymer or gold, the absence of any major holes or gaps in the film would indicate a nonporous membrane structure. The conclusion that can be drawn from Figure 2 is that the PPOP4A membrane is very dense, with a structure on the order of molecular dimensions. Additional SEM and TEM studies on films PPOP4B and PPOP4C are in progress and are expected to reveal a more open membrane structure.

Pure Gas Transport Characteristics. The transport behavior of PPOP4A and PPOP4B was examined at 25^{o}C and 1.59 bar as a function of test gas. The results of the time-lag studies on membrane PPOP4A are summarized in Figures 3 and 4. As a result of the errors estimated in the membrane time lags, a comparison of only the relative magnitudes of S and D for the different gases is valid (small differences in absolute values are insignificant). The permeability results shown in Figure 3 are plotted as a function of kinetic gas diameters (determined from gas viscosity data) (16,17). The experimental results are based on two separate experiments with the same membrane. The general trend of the PPOP transport behavior is the same for both experiments; permeability decreases with increasing molecular size. The one notable exception to the general trend in both experiments, however, is sulfur dioxide. This deviation is attributed to a high solubility of sulfur dioxide in the membrane.

Gas transport or permeation across a polymer membrane can be thought of as three discrete events: sorption into the membrane, diffusion through the membrane, and desorption out of the membrane. Sorption into and out of the membrane is related to solubility, and transport through the membrane is dependent on

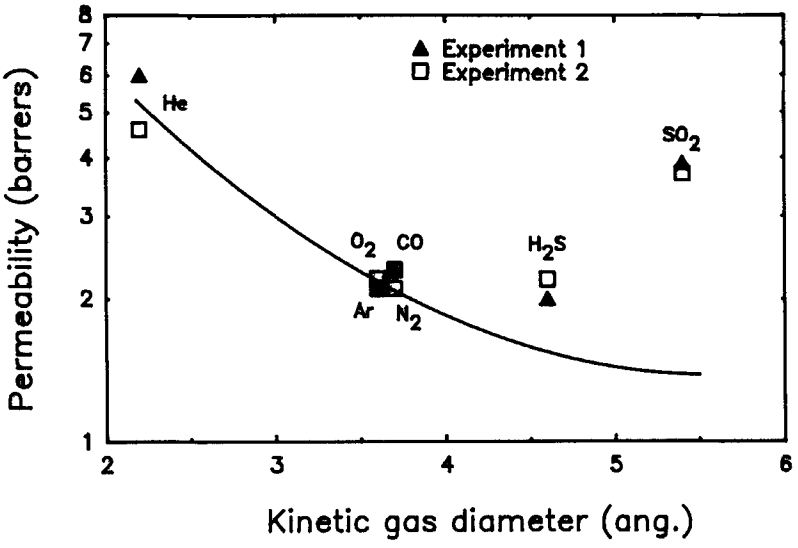

Figure 3.0 Gas permeability data for membrane PPOP4A (spin cast; solvent evaporation <5 s).

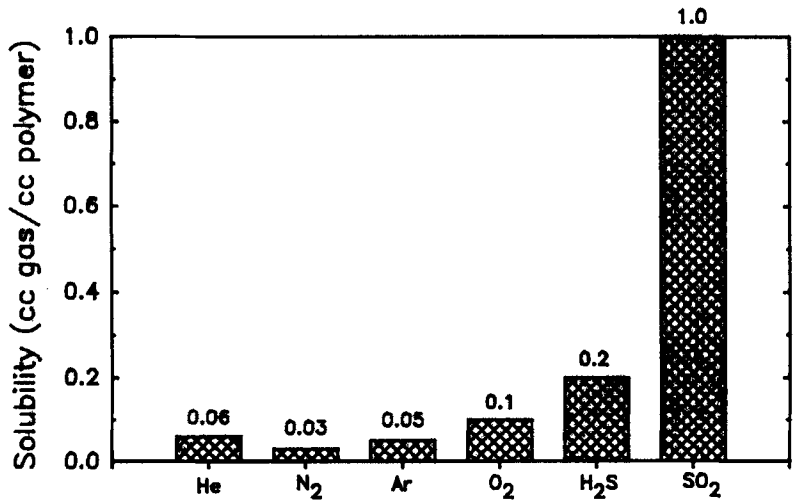

Figure 4.0 Gas solubility data for membrane PPOP4A (spin cast; solvent evaporation <5 s).

Table II. Comparison of permeability data from membrane PPOP4A and PPOP4B

Gas	Permeability (barrer)		Perm Ratio (P_{gas}/P_{He})	
	PPOP4A	PPOP4B	PPOP4A	PPOP4B
He	6.01	15.08	1.00	1.00
N_2	2.26	6.04	0.38	0.40
O_2	2.11	5.90	0.35	0.39
H_2S	1.96	11.98	0.33	0.80
Ar	2.07	5.18	0.34	0.34
SO_2	3.86	74.67	0.64	4.67*

* Based on P_{He} value of 16.0 barrers.

diffusion. Factors which affect gaseous diffusion primarily deal with the membrane microstructure and gas size. In the case of solubility, the gas/membrane and gas/gas physicochemical properties are important. In the absence of strong solubility effects, overall transport (permeability) is diffusion controlled and related to molecular size (13). This type of transport-size trend is typically observed with noble, atmospheric and nonpolar gases (6,13,18). The permeability size correlation of the gases helium, carbon monoxide, nitrogen, oxygen, argon, and hydrogen sulfide probably indicates that gas size was the controlling factor of transport through the membrane PPOP4A and that solubility factors were negligible. Since sulfur dioxide deviates from the expected diffusion controlled process, it is apparent that solubility factors are contributing to overall transport. PPOP4A gas solubilities determined from time-lag and permeability data are shown in Figure 4. The figure shows higher solubilities for SO_2, H_2S, and O_2 than for the faster diffusing gases He, N_2, and Ar. The SO_2 solubility result is significant since it is about 50 times more soluble in the membrane than other gases. This result confirms the assumption drawn from permeability data on sorption controlled transport.

The transport characteristics of the knife-cast membrane PPOP4B are summarized in Table II and Figures 5 and 6. Table II shows the permeabilities and permeability ratios for membranes PPOP4A and PPOP4B. This table, along with the permeability plot in Figure 5, shows two enhancement effects in the transport properties of PPOP4B. First, the permeabilities of all the gases were enhanced in PPOP4B by about 3-4 times over PPOP4A. This enhancement is expected for the more open membrane structure observed in the PPOP4B membrane. The other enhancement was an

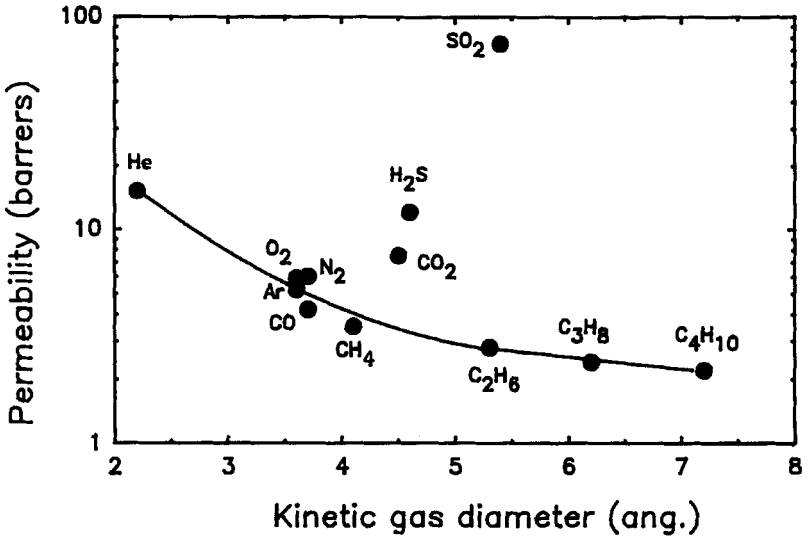

Figure 5.0 Gas permeability data for membrane PPOP4B (knife cast; solvent evaporation 30 min).

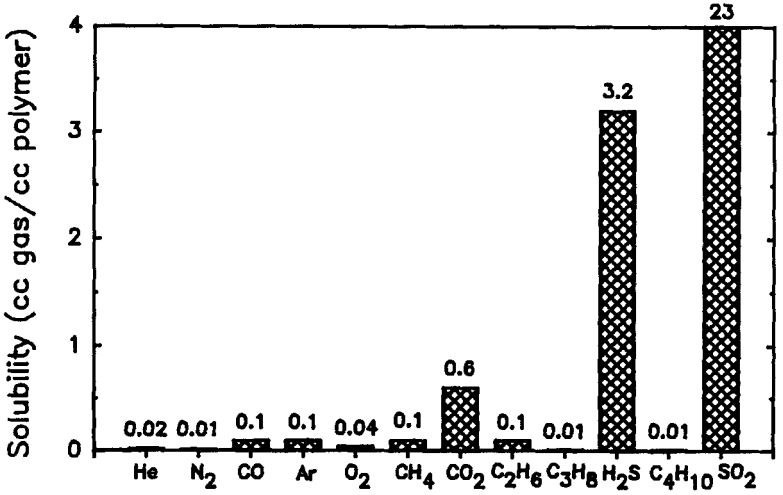

Figure 6.0 Gas solubility data for membrane PPOP4B (knife cast; solvent evaporation 30 min).

increase in selectivity (permeability ratio). In general, a loosening of polymer structure will lead to an increase in permeability but with a sacrifice in selectivity. One possible cause for this result would be an increase in soluble polymer volume for PPOP4B. The soluble polymer volume refers only to amorphous regions of the polymer since highly packed crystalline regions are generally considered to be insoluble. Gas solubility through amorphous regions could be increased in two ways in the present experiment: 1) by a decrease in percent crystallinity or 2) by a rearrangement of amorphous polymer to provide a higher local volume with the same overall amorphous percentage. Both DSC and X-ray diffraction studies are in progress to determine the validity of these arguments. However, it is suspected that the latter is true for the present study and directly related to the casting methodology (13). For the spin cast membrane, rapid evaporation results in a membrane matrix of small randomly oriented crystallites, depicted in Figure 2d. The amorphous regions surrounding these small crystallites would have a low local volume and have a uniform random distribution throughout the film. For long evaporation times, as in the case of the knife cast film, crystalline regions would grow, orient, and pack in order to attain lower free energy in the system. This would lead to the formation of larger structures. As a consequence of crystallite packing, the amorphous material would be concentrated between crystalline regions and provide a larger local amorphous volume for gas permeation, the result being an increase in diffusivity and solubility. Another effect of large membrane structure is the increase in apparent surface area and decrease in apparent thickness. This would also lead to an overall enhancement of permeability.

The permeability-gas diameter plot for PPOP4B is shown in Figure 5. The permeabilities of the hydrocarbon and atmospheric gases agree fairly well with predictions for diffusion controlled permeability; that is, permeability controlled by molecular size. The permeability of the remaining gases (carbon dioxide, hydrogen sulfide, and sulfur dioxide) appears to be controlled by solubility factors because of the deviation from the permeability-size trend. A significant enhancement in the permeability ratio is observed for SO_2 in film PPOP4B (shown in Table II). The solubility data for PPOP4B is shown in Figure 6. As expected, there is little difference in the solubility of the atmospheric and hydrocarbon gases where diffusion controlled transport was observed. The remaining gases (hydrogen sulfide, sulfur dioxide, and carbon dioxide) where the influence of solubility factors on transport is predicted, are, as expected, more soluble in PPOP4B membrane.

The transport characteristics of PPOP4A and PPOP4B complement each other in elucidating the mechanism for enhanced selectivity. As evidenced by Figures 3 and 5, the atmospheric and hydrocarbon gas transport behavior of both membranes

Table III. Comparison of solubility and diffusivity ratios.

Gas	Solubility Ratio (gas/He)		Diffusivity Ratio (gas/He)	
	PPOP4A	PPOP4B	PPOP4A	PPOP4B
He	1.0	1.0	1.0	1.0
N_2	0.5*	0.6*	0.9	0.7
O_2	2.0	3.0	0.2	0.1
Ar	0.7	6.0*	0.5	0.6
H_2S	3.0	200.0	0.1	0.1
SO_2	20.0	1000.0	<0.1	<0.1
CO_2	--	20.0	--	<0.1
CO	--	0.8	--	1.0
CH_4	--	1.0	--	0.6
C_2H_6	--	0.7	--	0.8
C_3H_8	--	0.1	--	6.0
C_4H_{10}	--	0.1	--	3.0

* - time lag errors suspected for unusually high or low values

correlates well with a permeability-size relationship, indicating a diffusion controlled transport process with negligible sorption. The transport of SO_2, H_2S, and CO_2 deviates from the permeability-size correlation. Based on the permeability equation ($P = DS$) this indicates the influence of solubility effects.

A comparison of solubility and diffusivity ratios for the two membranes is given in Table III. The overall permeability increase observed for PPOP4B in Table II is due to an increase in diffusion rate as the result of a more open membrane structure. Based on these data, it is concluded that the relative enhancement of SO_2, H_2S, and CO_2 permeability is due to solubility effects. In accordance with the permeability equation, the permeability ratio can also be represented as a product of a solubility ratio and diffusivity ratio. The diffusivity ratios for the two membranes are fairly constant, indicating little effect on the permeability ratio. Significant enhancements are observed in PPOP4B for the solubility ratios of SO_2 and H_2S. This, of course, indicates as previously stated that the selectivity enhancements reported for PPOP4B are the result of solubility effects.

CONCLUSIONS

Poly[bis(phenoxy)phosphazene] was successfully cast into dense homogeneous membrane films using solvent casting

techniques. Solvent evaporation rate was found to play an important role in determining the microstructure of the membrane. Spin casting techniques with rapid evaporation produced dense, homogeneous membranes with transparent structures. The knife casting techniques, which allowed for slower evaporation times, resulted in translucent to opaque membranes with more open structures; pores formed in the extreme case with evaporation times on the order of hours.

The following conclusions on gas transport through the PPOP membranes can be drawn from the time-lag gas permeation studies and polymer microstructural investigations.

- The pure gas transport of atmospheric and hydrocarbon gases through the PPOP membrane is a diffusion controlled process in which permeation rates correlate with molecular size; sorption effects are negligible.

- The pure gas transport of sulfur dioxide, hydrogen sulfide, and carbon dioxide deviates from the diffusion controlled permeability-size correlation. This indicates the influence of solubility factors.

- The transport properties of the knife cast membrane were enhanced in two respects from the dense spin cast membrane. An overall increase in permeability observed for all the test gases supports the results of the polymer morphology studies indicating a more open membrane structure. The increase in solubility ratios for gases with sorption controlled transport suggests an increase in overall amorphous polymer volume or redistribution to result in an increase of local amorphous volume.

ACKNOWLEDGMENT

The work described in this paper was supported by the Department of Interior's Bureau of Mines under Contract No. J0134035 through Department of Energy Contract No. DE-AC07-76ID01570. Special thanks is extended to Mr. T. E. Doyle for his valuable assistance in helping with the TEM and SEM studies.

REFERENCES

1) Leeper, S.A., et al., *Membrane Technology and Applications: An Assessment*, EG&G-2282, U.S. DOE Contract No. DE-AC07-76ID1570.

2) Allen, C.A., et al., *Strategic and Critical Materials Program Annual Report-1986*, BOM contract J0134035 (DOE-INEL), May 1986.

3) Allen, C.A., et al., *J. Membrane Sci. 33*, 181 (1987).

4) Allcock, H.R., *Phosphorus Nitrogen Compounds*, Academic Press Inc., New York, 1972.

5) Allcock, H.R., *Chem. Eng. News 63*, 22 (1985).

6) Wang, S.H. and Kammermeyer, K., *Techniques of Chemistry, Volume VII: Membranes in Separations*, Robert E. Kreiger Publ. Co., Malabar, Florida, 1984.

7) Barrer, R.M., *Trans. Faraday Society 35*, 628 (1939).

8) Van Amerongen, G.J., *J. Applied Physics 17*, 972 (1946).

9) Rogers, C, et al., *TAPPI 39(11)*, 737 (1956).

10) Singler R.E., et al., *J. Polym. Sci., Polym. Chem. Ed. 12*, 433 (1974).

11) McCaffrey, R.R., et al., *Separation Science and Technology 22*, 873 (1987).

12) ASTM Method D3593-77.

13) Kesting R.E., *Synthetic Polymeric Membranes, A Structural Perspective*, 2nd Edition, John Wiley & Sons, New York, 1985.

14) Maisel, L.I. and Glang, R., *Handbook of Thin Film Technology*, McGraw-Hill, New York, 1970.

15) Allcock, H.R., et al., *JACS 107*, 5166 (1985).

16) Michaels, A.S., Bixler, H.J., *J. Polym. Sci. 50*, 413 (1961).

17) *CRC Handbook of Chemistry and Physics, 57th edition*, CRC Press, Cleveland, Ohio, 1976, pp. F58-61.

18) Chern, R.T., et al., *Materials Science of Synthetic Membranes, ACS Symposium Series 269*, Lloyd, D.R. editor, ACS, Washington D.C., 1985, Ch. 2, pp. 25-46.